Protein Science (1999), *8*:518–528. Cambridge University Press. Printed in the USA.

Mapping cyclic nucleotide-induced conformational changes in cyclicAMP receptor protein by a protein footprinting technique using different chemical proteases

NOEL BAICHOO AND TOMASZ HEYDUK

Edward A. Doisy Department of Biochemistry and Molecular Biology, St. Louis University Medical School, 1402 S. Grand Blvd., St. Louis, Missouri 63104

(RECEIVED August 24, 1998; ACCEPTED December 1, 1998)

Abstract

CyclicAMP receptor protein (CRP) regulates transcription of numerous genes in *Escherichia coli*. Both cAMP and cGMP bind CRP, but only cAMP induces conformational changes that dramatically increase the specific DNA binding activity of the protein. We have shown previously that our protein footprinting technique is sensitive enough to detect conformational changes in CRP by cAMP [Baichoo N, Heyduk T. 1997. *Biochemistry 36*:10830–10836]. In this work, conformational changes in CRP induced by cAMP and cGMP binding were mapped and quantitatively analyzed by protein footprinting using iron complexed to diethylenetriaminepentaacetic acid ($[Fe\text{-}DTPA]^{2-}$), iron complexed to ethylenediaminediacetic acid ([Fe-EDDA]), iron complexed to desferrioxamine mesylate ($[Fe\text{-}HDFO]^{+}$), and copper complexed to *o*-phenanthroline ($[(OP)_2Cu]^{+}$) as proteases. These chemical proteases differ in size, charge, and hydrophobicity. Binding of cAMP to CRP resulted in changes in susceptibility to cleavage by all four proteases. Cleavage by [Fe-EDDA] and $[Fe\text{-}DTPA]^{2-}$ of CRP-cAMP detected hypersensitivities in the DNA-binding F α-helix, the interdomain hinge, and the ends of the C α-helix, which is involved in intersubunit interactions. [Fe-EDDA] and $[Fe\text{-}DTPA]^{2-}$ also detected reductions in cleavage in the D and E α-helices, which are involved in DNA recognition. Cleavage by $[Fe\text{-}HDFO]^{+}$ of CRP-cAMP detected hypersensitivities in β-strand 8, the B α-helix, as well as in parts of the F and C α-helices. $[Fe\text{-}HDFO]^{+}$ also detected protections from cleavage in β-strands 4 to 5 and their intervening loop, β-strand 7, which is part of the nucleotide binding pocket, as well as in the D and E α-helices. Cleavage by $[(OP)_2Cu]^{+}$ of CRP-cAMP detected hypersensitivities in β-strands 9 and 11 as well as in the D and E α-helices. $[(OP)_2Cu]^{+}$ also detected protections in the C α-helix , the interdomain hinge, and β-strands 2–7. Binding of cGMP to CRP resulted in changes in susceptibility to cleavage only by $[(OP)_2Cu]^{+}$, which detected minor protections in β-strands 3–7, the interdomain hinge, and the C α-helix. These results show that binding of cAMP causes structural changes in CRP in the nucleotide binding domain, the interdomain hinge, the DNA binding domain, and regions involved in intersubunit interaction. Structural changes induced by binding of cGMP appear to be very minor and confined to the nucleotide binding domain, the interdomain hinge, and regions involved in intersubunit interaction. Use of different cleaving agents in protein footprinting seems to give a more detailed picture of structural changes than the use of a single protease alone.

Keywords: copper chelates cyclicAMP receptor protein; iron chelates; protein conformational changes; protein footprinting

CyclicAMP receptor protein (CRP) regulates transcription of over 100 genes in *Escherichia coli* (for recent reviews, see Kolb et al., 1993; Adhya et al., 1995). CRP consists of a homodimer, each subunit of which is comprised of a N-terminal and a C-terminal domain connected by a hinge region as shown in Figure 1. Upon binding cAMP, CRP undergoes a conformational change that allows it to bind specific DNA sequences with increased affinity (Krakow & Pastan, 1973; Wu & Wu, 1974; Wu et al., 1974; Eilen & Krakow, 1977; Pampeno & Krakow, 1979; Tsugita et al., 1982; Ebright et al., 1985; Heyduk & Lee, 1989; DeGrazia et al., 1990; Lee et al., 1990; Sixl et al., 1990; Tan et al., 1991; Hinds et al., 1992). CRP can also bind cGMP; however, this ligand does not improve specific binding of the protein to DNA (Takahashi et al., 1980; Fried & Crothers, 1984). The structural basis for the increased DNA binding activity of CRP induced by cAMP is not fully understood. Crystal structures of cAMP and DNA-bound CRP

Reprint requests to: Tomasz Heyduk, Edward A. Doisy Department of Biochemistry and Molecular Biology, St. Louis University Medical School, 1402 S. Grand Blvd., St. Louis, Missouri 63104; e-mail: heydukt@wpogate.slu.edu.

Abbreviations: cAMP, cyclic 3′,5′-adenosine monophosphate; cGMP, cyclic 3′,5′-guanosine monophosphate; CRP, cAMP receptor protein; $CRP^{\#}$, a derivative of CRP labeled at the N-terminus with P^{33}; DTPA, diethylenetriaminepentaacetic acid; EDDA, ethylenediaminediacetic acid; HDFO, desferrioxamine mesylate; HMPK, heart muscle protein kinase; OP, *o*-phenanthroline; RNAP, RNA polymerase.

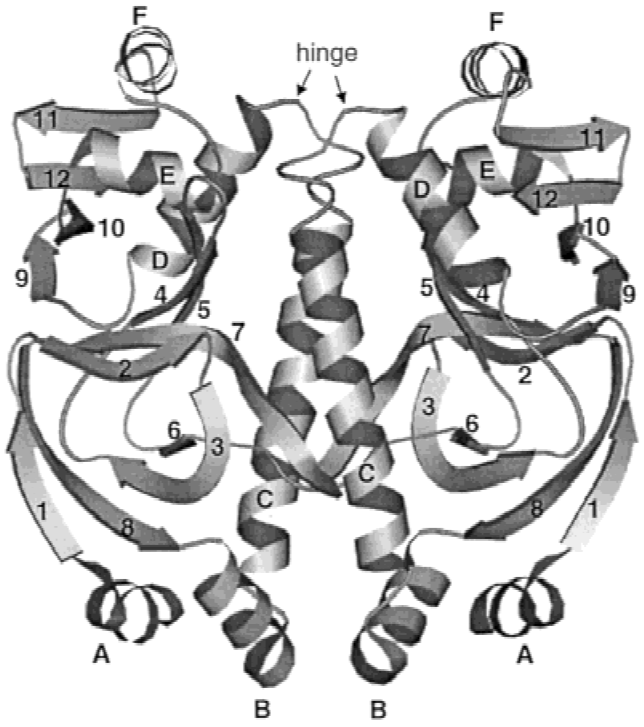

Fig. 1. Structure of the CRP dimer. The six α-helices are lettered, the 12 β strands are numbered, and the interdomain hinge is labeled. The figure was drawn with MOLSCRIPT (Kraulis, 1991) using coordinates for CRP in the cAMP–CRP–DNA complex (Parkinson et al., 1996). The coordinates were obtained from the Brookhaven Protein Data Bank (accession code 1BER). Secondary structures were assigned as described by Weber and Steitz (1987).

are known (McKay et al., 1982; Weber & Steitz, 1987; Schultz et al., 1991; Parkinson et al., 1996). However, no three-dimensional structure of unliganded CRP is available. In the absence of structural data, models of cAMP-induced conformational transition in CRP were proposed on the basis of mutagenesis data (Garges & Adhya, 1985, 1988; Kim et al., 1992). According to these models, binding of cAMP to the N-terminal domain induces a rearrangement of DNA-binding α-helices in the C-terminal domain of the protein. Energetic studies on intersubunit and interdomain interactions in CRP and its mutants provided evidence that both intersubunit and interdomain interactions play a role in a cAMP-dependent conformational switch in CRP (Cheng et al., 1993, 1995; Cheng & Lee, 1998). These studies suggest that multiple regions of the protein should be affected by cAMP binding.

We have shown recently that our protein footprinting technique (Heyduk & Heyduk, 1994; Heyduk et al., 1996) can be used to map regions of protein affected by conformational changes (Baichoo & Heyduk, 1997). In this protein footprinting technique, regions of protein involved in conformational changes upon ligand binding can be identified by changes in susceptibility to a protease. Identification of cleavage products is achieved by using an end-labeled protein whose fragments are separated by electrophoresis. Development of quantitative methods for the analysis of these data has allowed detection of small changes in sensitivity of protein to cleavage and high-resolution mapping (Heyduk et al., 1996). These previous protein footprinting studies used $[\text{Fe-EDTA}]^-$ as a protease. However, several other metal complexes varying in size, charge, and hydrophobicity can also be used as chemical proteases. Different proteases may recognize and cleave different protein motifs and, thus, should be able to detect different but complementary aspects of the same structural change. Assembling the regions of CRP identified by each protease as being perturbed by cAMP should give a more complete picture of structural changes that occur. Additionally, comparing the results between proteases gives information on their specificity and on what aspects of conformational change each recognizes.

In this work we map conformational changes induced in CRP upon cAMP and cGMP binding using protein footprinting with four metal–chelate complexes. The regions in CRP affected by cyclic nucleotide binding were identified as those where changes in sensitivity to cleavage by metal–chelate complexes were observed.

Results

In our experiments we have used a CRP protein that has seven nonnative amino acids at the N-terminus and eight nonnative amino acid residues at the C-terminus. We have previously shown that the additional nonnative amino acid residues did not significantly perturb the conformation of CRP because this modified protein is as active as the wild-type (wt) protein in binding cAMP, specific DNA sequences, and RNA polymerase (RNAP) (Baichoo & Heyduk, 1997). After specific labeling of the the N-terminus with ^{33}P, the protein (referred to as CRP$^{\#}$) was subjected to limited cleavage with proteases in the presence and absence of cAMP and cGMP. Cleavage reactions were performed under "single hit" conditions (Brenowitz et al., 1986), in which less than 10% of the protein was cut. The products of cleavage reactions were resolved using denaturing gel electrophoresis (Schagger & von Jagow, 1987), and examples of autoradiograms of these gels are shown in Figures 2A–5A. The bands of cleavage products were assigned by comparing their electrophoretic mobility with the mobility of appropriate standards (Materials and methods; Baichoo & Heyduk, 1997). Although differences between gel lanes can be detected visually (Figs. 2A–5A), data were subjected to rigorous quantitative analysis (Heyduk et al., 1996; Baichoo & Heyduk, 1997), and are presented as difference plots that graph the normalized difference between gel lanes vs. amino acid sequence (Figs. 2–5). Positive values of normalized difference correspond to regions of CRP$^{\#}$ that become hypersensitive to cleavage by protease upon binding cyclic nucleotide, while negative values correspond to regions that become protected from cleavage. Protections and hypersensitivities were considered significant if greater in magnitude than $2\times$ the standard error, which is shown as the error bar to the left of each plot (Figs. 2B–5B). Relevant secondary structural motifs of CRP are shown in difference plots as lines above regions where significant changes occur. All secondary structure elements of CRP are shown in Figure 1, where they are identified using the same labels as used in Figures 2–5.

Changes in susceptibility of CRP$^{\#}$ to cleavage by $[\text{Fe-DTPA}]^{2-}$ upon binding cyclic nucleotides

Figure 2A shows a gel image of a protein footprinting experiment in which CRP$^{\#}$, CRP$^{\#}$-cAMP, and CRP$^{\#}$-cGMP are subjected to limited proteolysis by $[\text{Fe-DTPA}]^{2-}$. Major differences in band intensities were seen between lanes corresponding to CRP$^{\#}$ and CRP$^{\#}$-cAMP, but not between lanes corresponding to CRP$^{\#}$ and CRP$^{\#}$-cGMP. Differences in band intensities were observed pri-

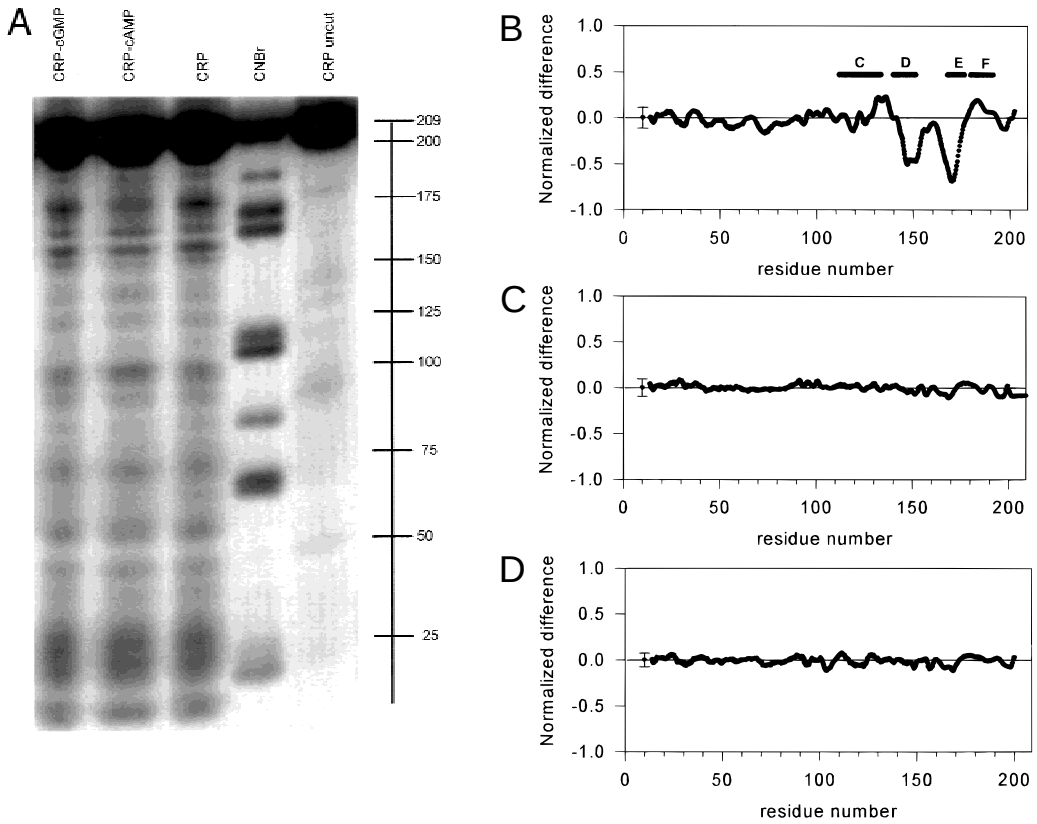

Fig. 2. $[Fe\text{-}DTPA]^{2-}$ cleavage of $CRP^{\#}$ and its complexes with cAMP and cGMP. **A:** Autoradiogram of a protein footprinting SDS-PAGE for $CRP^{\#}$ and its complexes with cAMP and cGMP, using $[Fe\text{-}DTPA]^{2-}$ as a cleaving reagent. The lane labeled CRP uncut was loaded with $CRP^{\#}$ untreated by $[Fe\text{-}DTPA]^{2-}$, while the lane labeled CNBr was loaded with $CRP^{\#}$ partly digested by CNBr. All other lanes are loaded with free $CRP^{\#}$ and its complexes with cAMP and cGMP as labeled subjected to $[Fe\text{-}DTPA]^{2-}$-mediated cleavage. **B**–**D**: Averaged difference plots showing results of quantitative analysis of multiple experiments shown in **A**. Normalized difference is defined as $(I - I_{CRP\#})/I$, where I is the corrected Phosphorimager intensity for the complex under study and $I_{CRP\#}$ is the corrected Phosphorimager intensity for $CRP^{\#}$ alone. **B**: Averaged difference plot for the cAMP–$CRP^{\#}$ complex vs. $CRP^{\#}$. **C:** Averaged difference plot for $CRP^{\#}$ vs. $CRP^{\#}$. **D:** Averaged difference plot for the cGMP–$CRP^{\#}$ complex vs. $CRP^{\#}$.

marily in the C-terminal region of the protein. Figure 2B shows a difference plot (average of results from four gels) for cAMP binding to $CRP^{\#}$. Upon binding cAMP, major protections were observed in amino acid residues 142–157 and 162–175, which correspond to the D and E α-helices, respectively. Hypersensitivity upon binding cAMP was observed in residues 130–137, which correspond to part of the C α-helix and the interdomain hinge, and in residues 180–185, which correspond to part of the F α-helix. Figure 2C shows a difference plot of unliganded $CRP^{\#}$ in which no significant changes in susceptibility were observed, demonstrating that data analysis introduced no systematic errors. No significant changes in susceptibility of CRP to $[Fe\text{-}DTPA]^{2-}$ were detected upon binding cGMP, as shown in Figure 2D. Results obtained using $[Fe\text{-}DTPA]^{2-}$ are very similar to those obtained previously using $[Fe\text{-}EDTA]^{-}$ as a chemical protease (Baichoo & Heyduk, 1997).

Changes in susceptibility of $CRP^{\#}$ to cleavage by [Fe-EDDA] upon binding cyclic nucleotides

Figure 3A shows a gel image of a protein footprinting experiment in which $CRP^{\#}$, $CRP^{\#}$-cAMP, and $CRP^{\#}$-cGMP were subjected to limited proteolysis by [Fe-EDDA]. As in the case of $[Fe\text{-}DTPA]^{2-}$, differences in corresponding band intensities were observed between $CRP^{\#}$ and $CRP^{\#}$-cAMP, but not between $CRP^{\#}$ and $CRP^{\#}$-cGMP. Most changes were observed in the C-terminal region of the protein. Figure 3B shows that major protections from cleavage by [Fe-EDDA] upon binding cAMP occurred in residues 141–156 and 164–179, which corresponded to the D and E α-helices, respectively. Residues 109–114, which correspond to parts of the B and C α-helices; residues 130–137, which correspond to parts of the C α-helix and interdomain hinge; and residues 183–186, which correspond to the F α-helix, all became hypersensitive to cleavage by [Fe-EDDA] upon binding cAMP. Figure 3C shows a difference plot of unliganded $CRP^{\#}$ in which no significant changes in susceptibility were seen. Figure 3D shows that [Fe-EDDA] did not detect any changes in susceptibility of CRP upon binding cGMP. Results from cleavage of CRP by the uncharged [Fe-EDDA] parallel those observed using negatively charged $[Fe\text{-}DTPA]^{2-}$, indicating that the two iron chelate complexes have similar modes of recognition and cleavage of polypeptides.

Changes in susceptibility of $CRP^{\#}$ to cleavage by $[Fe\text{-}HDFO]^{+}$ upon binding cyclic nucleotides

Figure 4A shows a gel image of a protein footprinting experiment in which $CRP^{\#}$, $CRP^{\#}$-cAMP, and $CRP^{\#}$-cGMP were subjected to

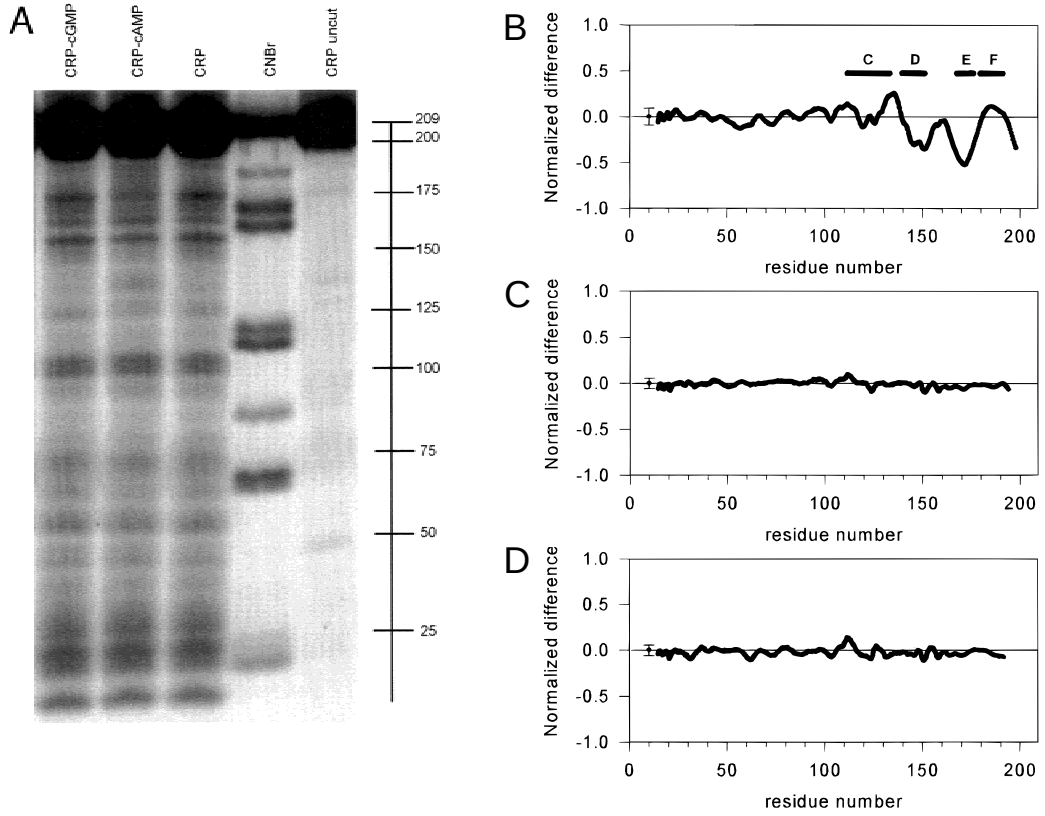

Fig. 3. [Fe-EDDA] cleavage of CRP$^{\#}$ and its complexes with cAMP and cGMP. **A:** Autoradiogram of a protein footprinting SDS-PAGE for CRP$^{\#}$ and its complexes with cAMP and cGMP using [Fe-EDDA] as a cleaving reagent. Lanes are labeled as in Figure 2. **B:** Averaged difference plot for the cAMP–CRP$^{\#}$ complex vs. CRP$^{\#}$. **C**: Averaged difference plot for CRP$^{\#}$ vs. CRP$^{\#}$. **D**: Averaged difference plot for cGMP–CRP$^{\#}$ complex vs. CRP$^{\#}$.

limited proteolysis by $[\text{Fe-HDFO}]^{+}$. Visual examination of the gel image reveals major differences between CRP$^{\#}$ and CRP$^{\#}$-cAMP, but not between CRP$^{\#}$ and CRP$^{\#}$-cGMP. Differences in band intensities are seen in both the N- and C-terminal domains. Figure 4B shows a difference plot resulting from the averaging of seven gels. Some differences in band intensities between lanes in the single gel shown in Figure 4A became attenuated in Figure 4B due to averaging of data from multiple experiments. On the basis of Figure 4B, significant protections of CRP from cleavage by $[\text{Fe-HDFO}]^{+}$ upon binding cAMP were seen in residues 48–60, which correspond to β-strands 4 to 5 and their intervening loop; residues 82–88, which correspond to β-strand 7; residues 148–155, which correspond to the D α-helix; and residues 168–181, which correspond to the E α-helix. Hypersensitivity to cleavage upon binding cAMP was observed in residues 96–102, which correspond to β-strand 8; residues 131–140, which correspond to part of the C α-helix and interdomain hinge; and residues 184–197, which correspond to the F α-helix. Figure 4C and 4D show no significant changes in susceptibility for unliganded CRP and CRP-cGMP, respectively. Cleavage of CRP-cAMP by $[\text{Fe-HDFO}]^{+}$ detected aspects of cAMP-induced conformational changes in the N-terminal domain that were not observed when $[\text{Fe-DTPA}]^{2-}$ and [Fe-EDDA] were used as proteases; namely, protections from cleavage in β-strands 4 to 5 and 7, and hypersensitivity of β-strand 8. These observations suggest that recognition and cleavage of proteins by $[\text{Fe-HDFO}]^{+}$ is different from that of $[\text{Fe-DTPA}]^{2-}$ and [Fe-EDDA], and that minor structural changes may occur in the N-terminal region of CRP upon binding cAMP. Changes in susceptibility in the C-terminal domain of CRP upon binding cAMP are similar for $[\text{Fe-HDFO}]^{+}$, $[\text{Fe-DTPA}]^{2-}$, and [Fe-EDDA]. These changes all map reductions in accessibility of the D and E α-helices and increased accessibility of the C and F α-helices as well as the interdomain hinge. Thus, in spite of their different charges and possibly different modes of proteolysis, all three iron–chelate complexes detected major conformational changes in CRP upon binding cAMP.

Changes in susceptibility of CRP to $[(OP)_2Cu]^{+}$ upon binding cyclic nucleotides

Figure 5A shows a gel image of an experiment in which CRP$^{\#}$ was subjected to cleavage by $[(OP)_2Cu]^{+}$ in the presence and absence of cyclic nucleotides. In the absence of nucleotides, a preferred site of cleavage was observed. A major band ~125 was observed that corresponded to the C α-helix. Sensitivity of CRP$^{\#}$ to cleavage by $[(OP)_2Cu]^{+}$ changes in the presence of each cyclic nucleotide. Upon binding cAMP, a dramatic reduction in intensity was observed in parts of gels corresponding to amino acid residues 112–135, while lesser reductions were seen in regions corresponding to the N-terminal region of the protein. In some experiments, reductions were also observed in the C-terminal regions; however, these disappeared upon averaging multiple experiments. Minor increases

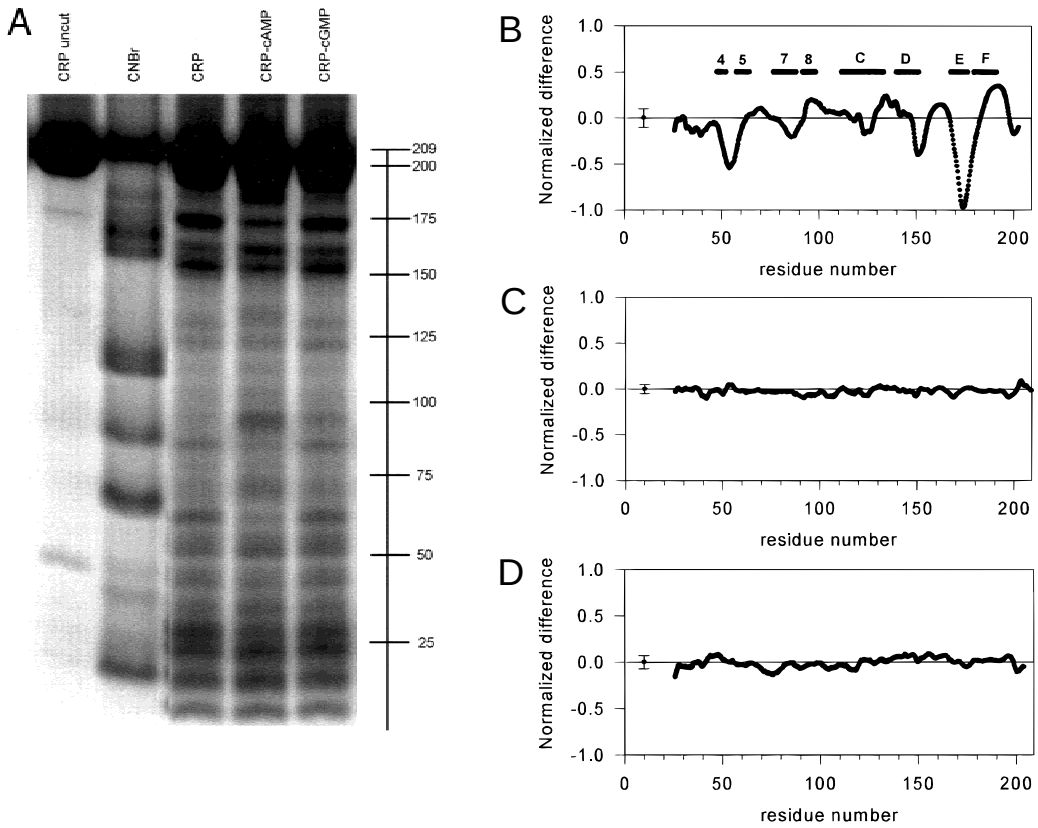

Fig. 4. $[Fe\text{-}HDFO]^+$ cleavage of $CRP^{\#}$ and its complexes with cAMP and cGMP. **A:** Autoradiogram of a protein footprinting SDS-PAGE for $CRP^{\#}$ and its complexes with cAMP and cGMP using $[Fe\text{-}HDFO]^+$ as a cleaving reagent. Lanes are labeled as in Figure 2. **B:** Averaged difference plot for the cAMP–$CRP^{\#}$ complex vs. $CRP^{\#}$. **C:** Averaged difference plot for $CRP^{\#}$ vs. $CRP^{\#}$. **D**: Averaged difference plot for the cGMP–$CRP^{\#}$ complex vs. $CRP^{\#}$.

in intensity were observed in regions of gels corresponding to the C-terminal domain. Figure 5B displays the results of seven gels averaged as a difference plot. After averaging results of multiple experiments, the major reduction in intensity between residues 113 and 138 is found to persist. This massive protection includes the long C α-helix and interdomain hinge. Minor protections that survived averaging were observed in residues 27–32, 35–38, 43–48, 53–62, and 63–84, which encompass β-strands 2–7. After averaging, minor hypersensitivities were noted in residues 147–175 as well as in residues 191–199. These regions of hypersensitivity include β-strands 9 and 11, and parts of the D, E, and F α-helices. Reductions in susceptibility to proteolysis can be attributed to conformational changes that disrupt cleavage sites for $[(OP)_2Cu]^+$. Conversely, enhancements of cleavage can be attributed to conformational changes that produce sites conductive to cleavage by $[(OP)_2Cu]^+$. Figure 5C shows a control data analysis showing no significant deviations from zero baseline in difference plot for unliganded $CRP^{\#}$.

Upon binding cGMP, changes in band intensities relative to free $CRP^{\#}$ were observed, as shown in Figure 5D. Reductions of band intensities in the N-terminal, but not C-terminal domain are in similar places to those observed upon formation of $CRP^{\#}$-cAMP. Figure 5D shows a difference plot averaged from multiple experiments. Protections from cleavage in the presence of cGMP were observed in residues 44–46, 52–61, and 62–83, which correspond to β-strands 2–7; residues 114–140, which correspond to the C α-helix and the interdomain hinge; and residues 184–191, which correspond to the F α-helix. Residues in β-strands 2–7, the C α-helix, and hinge region are protected from cleavage by $[(OP)_2Cu]^+$ upon binding cAMP and cGMP, indicating that some of the same domains of CRP are involved in structural changes induced by both ligands. However, the magnitudes of protection due to cAMP were generally smaller compared to cGMP, implying that the same regions of CRP may undergo different structural changes upon binding each ligand. Also, hypersensitivities in the C-terminal domain seen in the presence of cAMP were not observed in the presence of cGMP. Taken together, data from $[(OP)_2Cu]^+$ cleavage indicates that similar N-terminal regions of CRP are affected by interactions with cAMP and cGMP, but the conformational changes in these regions as well as those in the C α-helix, the interdomain hinge, and the C-terminal domain are different. This is consistent with both cyclic nucleotides being able to bind CRP in the N-terminal region, but only cAMP being able to improve DNA binding in the C-terminal region. Proteolysis by $[(OP)_2Cu]^+$ detects some aspects of conformational change that are not detected by the iron–chelate complexes, and vice versa. However, the combined results from all the chemical proteases used give a comprehensive picture of the conformational change that CRP undergoes upon binding cyclic nucleotides.

Discussion

Previous studies have established that binding of cAMP induces conformational changes in CRP, which improve the affinity of the

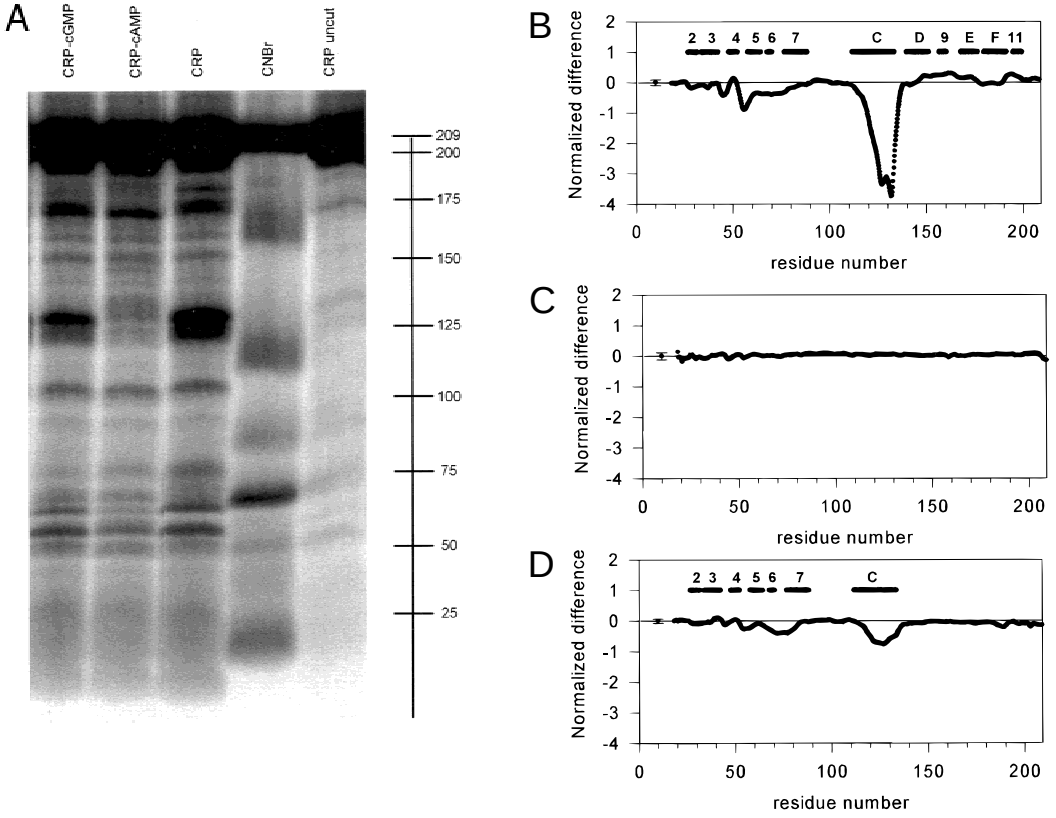

Fig. 5. $[(OP)_2Cu]^+$ cleavage of CRP$^{\#}$ and its complexes with cAMP and cGMP. **A:** Autoradiogram of a protein footprinting SDS-PAGE for CRP$^{\#}$ and its complexes with cAMP and cGMP using $[(OP)_2Cu]^+$ as a cleaving reagent. Lanes are labeled as in Figure 2. **B**: Averaged difference plot for the cAMP–CRP$^{\#}$ complex vs. CRP$^{\#}$. **C:** Averaged difference plot for CRP$^{\#}$ vs. CRP$^{\#}$. **D:** Averaged difference plot for the cGMP–CRP$^{\#}$ complex vs. CRP$^{\#}$.

protein for specific DNA sequences, while binding of cGMP does not (Takahashi et al., 1980). Using results from mutagenesis studies, a model has been proposed in which cAMP-binding induces a structural rearrangement of the interdomain hinge such that the F α-helix moves outward from the rest of the protein, allowing it to contact the major groove of DNA (Garges & Adhya, 1985). This model was supported by protein footprinting experiments using $[\text{Fe-EDTA}]^-$ as a protease (Heyduk & Heyduk, 1994; Baichoo & Heyduk, 1997). The current studies were performed to determine whether other chemical proteases differing in charge, size, and hydrophobicity would detect other aspects of cyclic nucleotide-induced conformational change. Additionally, such studies would provide information about the utility of the different proteases for protein footprinting.

Regions of CRP that experience significant changes in susceptibility to cleavage by iron–chelate complexes upon binding cAMP are shown in Figure 6, in which the CRP dimer is oriented as in Figure 1. Comparison of the panels in Figure 6 shows that protections of α-helices D and E as well as hypersensitivity of the F α-helix and interdomain hinge are detected by all three iron–chelate complexes used in this study. Figure 6B shows that [Fe-EDDA] also detected hypersensitivity in the N-terminus of the C α-helix. In addition to the changes detected by $[\text{Fe-DTPA}]^{2-}$ and [Fe-EDDA], cleavage by $[\text{Fe-HDFO}]^+$ detected protections in the loop between β-strands 4 to 5 which, although distant in the primary structure, is close to parts of α-helices D and E in the same subunit and the interdomain hinge of the other subunit in the three-dimensional structure (Fig. 1). Cleavage by $[\text{Fe-HDFO}]^+$ also detected a minor protection in β-strand 7 and minor hypersensitivities in β-strand 8 and the B α-helix, none of which were seen when the other iron–chelate complexes were used.

Hypersensitivity of the F α-helix detected previously using $[\text{Fe-EDTA}]^-$ agrees with the model proposed by Garges and Adhya (1988) that this region, upon binding of cAMP, moves away from the rest of the protein and becomes available for interaction with DNA. Hypersensitivity of the interdomain hinge indicates that it becomes rearranged upon binding cAMP, also in agreement with the model. Increased accessibility of this region to enzymatic proteases was observed previously (Krakow & Pastan, 1973; Tsugita et al., 1982; Angulo & Krakow, 1985; Ebright et al., 1985; Heyduk & Lee, 1989). Hypersensitivity of the ends of the C α-helix, which are involved in intersubunit interactions (McKay et al., 1982; Weber & Steitz, 1987), indicates that these regions may play a role in communicating structural changes induced by cAMP-binding in the N-terminal domain to the DNA-binding C-terminal domain. Reductions in susceptibility of α-helices D and E indicate that, upon binding cAMP, these regions undergo structural changes that may move them inward toward the body of the protein, thus making them less accessible to cleavage. Movement of the D α-helix inward toward the C α-helix has been proposed previously on the basis of mutagenesis studies in which interactions between residue 141 in the D α-helix and residue 138 in the hinge were shown to

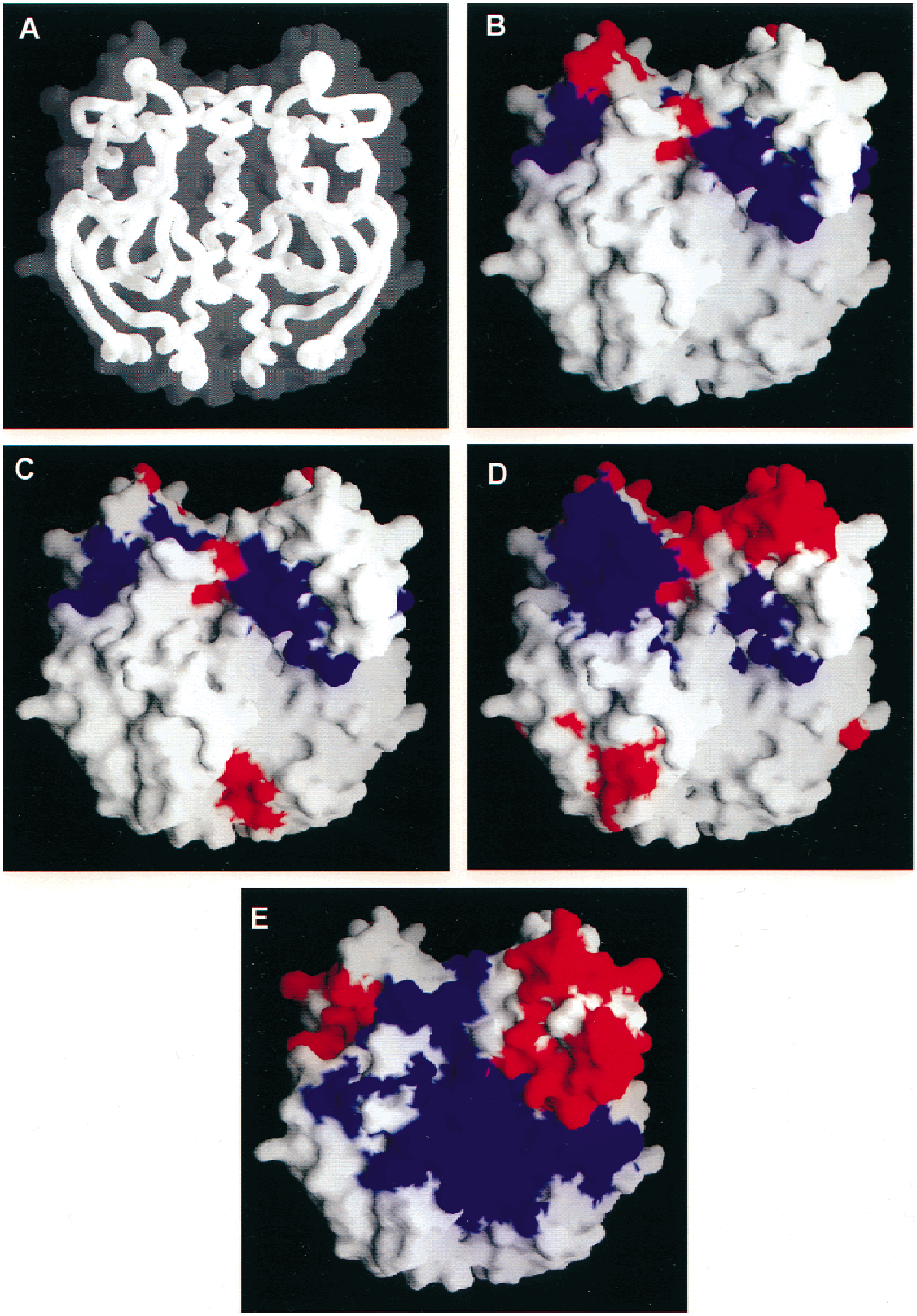

Fig. 6. Regions of CRP affected by binding of cAMP. The protein is in the same orientation as in Figure 1. **A:** The protein backbone superimposed on the surface. **B–E:** These correspond to surfaces illustrating results using $[\text{Fe-DTPA}]^{2-}$ (**B**), [Fe-EDDA] (**C**), $[\text{Fe-HDFO}]^{+}$ (**D**), and $[(\text{OP})_2\text{Cu}]^{+}$ (**E**), respectively. Red surfaces indicate areas of CRP that become more susceptible to cleavage in the presence of cAMP, while blue surfaces show areas that become less susceptible in the presence of cAMP. The figure was drawn with GRASP (Nicholls et al., 1991) using cAMP–CRP coordinates for the cAMP–CRP–DNA complex (Parkinson et al., 1996). The coordinates were obtained from Brookhaven Protein Data Bank (accession code 1BER).

affect the cAMP dependence of DNA binding by CRP (Kim et al., 1992; Ryu et al., 1993). Also, mutations of residues 169 and 171 in the E α-helix restore cAMP control to a cAMP independent *crp** mutant Ala144Thr suggesting a role for these interdomain interactions in the cAMP-induced conformational change (Garges & Adhya, 1988). Proteolysis by $[\text{Fe-HDFO}]^+$ detected protections in β-strands 4 to 5 and 7. The loop between β-strands 4 and 5 has been implicated in binding a second cAMP molecule in a recent DNA-bound structure of CRP (Passner & Steitz, 1997). Also, the loop between β-strands 4 and 5 of each subunit is in close proximity to the interdomain hinge of the other subunit; thus, rearrangements in the hinge could affect the susceptibility of the loop to some proteases. Parts of β-strand 7 are close enough to cAMP in the N-terminal binding pocket to form hydrogen bonds to cAMP (Weber & Steitz, 1987), and this region may undergo a slight rearrangement upon ligand binding. Minor hypersensitivities in β-strand 8 and the B α-helix, which connect the β-roll to the long C α-helix, are detected, indicating that a slight perturbation of these structures occurs upon cAMP binding. Results from the iron–chelate complexes in this study give a picture of major structural changes occurring in the C-terminal domain of CRP upon cAMP binding with minor structural perturbations in the N-terminal domain. None of the iron chelate complexes used in this study detected structural changes in CRP induced by binding cGMP. This is consistent with the inability of this cyclic nucleotide to induce DNA binding (Takahashi et al., 1980), and indicates that any conformational changes thus induced are very small in magnitude.

Figure 6D shows the localization of changes in susceptibility of CRP to cleavage by $[(\text{OP})_2\text{Cu}]^+$. Changes in susceptibility occur in both the N- and C-terminal domains upon binding cAMP. The most prominent change induced by cAMP was a dramatic reduction in susceptibility of CRP$^{\#}$ that almost exactly corresponds to the C α-helix and interdomain hinge. This indicates that binding of cAMP induces a structural change that makes the C α-helix and hinge less accessible to cleavage by $[(\text{OP})_2\text{Cu}]^+$. The long C α-helix is involved in cAMP binding as well as intersubunit interactions (Weber & Steitz, 1987). Changes in susceptibility of the C α-helix upon formation of CRP-cAMP are consistent with intersubunit interactions being important in conducting structural changes from the N-terminal region of CRP to the C-terminal region (Cheng et al., 1993; Cheng & Lee, 1998). Changes in susceptibility of the interdomain hinge region are consistent with this region being rearranged in the presence of cAMP. Smaller protections from cleavage were observed in the loops between β-strands 3 to 4 and 4 to 5 as well as in β-strands 5, 6, and 7. These regions all are part of the β-roll structure that binds cAMP. Parts of β-strands 6 and 7 are close enough to cAMP in the crystal structure to form hydrogen bonds (Weber & Steitz, 1987). The loop between β-strands 4 and 5 of each subunit is close to the interdomain hinge of the other subunit and to α-helices D and E of the same subunit and may be perturbed by rearrangements in these regions as well as by binding of a second cAMP molecule itself in the C-terminal domain of the protein (Passner & Steitz, 1997). Binding of cAMP to CRP may thus cause a perturbation of the nucleotide-binding β-roll, which abolishes cleavage sites for $[(\text{OP})_2\text{Cu}]^+$ in regions where protections were observed. Also, the loop between β-strands 4 and 5 may be part of a surface that, along with the hinge, presents cleavage sites for $[(\text{OP})_2\text{Cu}]^+$ that become disrupted upon binding of cAMP. Mild hypersensitivities occurred in β-strands 9 and 11 as well as in the D, E, and F α-helices upon binding cAMP. This observation indicates that these regions undergo a structural change in the presence of cAMP that produces sites more favorable to cleavage by $[(\text{OP})_2\text{Cu}]^+$. Taken together, changes in susceptibility of CRP to cleavage by $[(\text{OP})_2\text{Cu}]^+$ suggest that binding of cAMP perturbs elements of the β-roll structure as well as the C α-helix, and results in a reorientation of the interdomain hinge and rearrangement of secondary structural elements of the C-terminal region of CRP. This is entirely consistent with predictions made on the basis of detailed mutagenesis studies (Garges & Adhya, 1988) and in agreement with results from the iron–chelate complexes in this study. Comparison of Figures 2A–4A and Figure 5A shows that $[(\text{OP})_2\text{Cu}]^+$ produces different cleavage patterns from the iron–chelates. $[(\text{OP})_2\text{Cu}]^+$ seems to cleave intensely at very specific locations, allowing small structural changes in these regions to be detected. Although different changes in cleavage patterns were observed when the iron–chelate complexes and $[(\text{OP})_2\text{Cu}]^+$ were used, all identified the C, D, E, and F α-helices, and the interdomain hinge as sites of rearrangement upon cAMP binding. Additionally, $[(\text{OP})_2\text{Cu}]^+$ and $[\text{Fe-HDFO}]^+$ detected changes in the N-terminal domain of CRP upon cAMP binding.

None of the iron–chelate complexes used detected any conformational changes induced by cGMP. Small changes, however, were detected by $[(\text{OP})_2\text{Cu}]^+$, indicating the utility of this protease in detecting small perturbations in the protein structure. Figure 5D shows a difference plot illustrating changes in susceptibility of CRP to cleavage by $[(\text{OP})_2\text{Cu}]^+$ upon binding cGMP. Protections from cleavage occurred in β-strands 3–7 as well as in the C α-helix and interdomain hinge. Binding of cGMP appears to produce structural changes that abolish cleavage sites for $[(\text{OP})_2\text{Cu}]^+$ in β-strands 3–7. These regions are part of a nucleotide-binding β-roll structure where cGMP could reside in a CRP-cGMP complex. Binding of cGMP appears to induce structural changes in the C-α helix, reducing its susceptibility to $[(\text{OP})_2\text{Cu}]^+$. The central part of the C α-helix is also involved in binding cyclic nucleotides. Together, β-strands 3–7 and the C α-helix could be perturbed directly by binding of cGMP. The interdomain hinge, which is C-terminal to the C α-helix, also appears to undergo a structural change that increases its resistance to cleavage. Alternatively, a cGMP molecule could also be bound in the C-terminal domain of the protein and perturb residue 135 in the hinge as cAMP does in a recent DNA-bound structure of CRP (Passner & Steitz, 1997). Collectively, changes in susceptibility of CRP upon binding cGMP indicate that this cyclic nucleotide perturbs the β-roll structure and C α-helix, where it binds as well as the interdomain hinge where allosteric change or direct binding may occur. From an X-ray–derived structure of CRP-cAMP, parts of β-strands 6 and 7 interact with the ribose moiety, while parts of the C α-helix interact with the adenine moiety (Weber & Steitz, 1987). Both cyclic nucleotides used have ribose moieties; however, the purine bases differ. The differences between changes in susceptibility of the C α-helix to cleavage in the presence of each cyclic nucleotide suggests that the interaction between the C α-helix and purine moiety may be important in effecting the initial conformational change.

Results from proteolysis by $[\text{Fe-DTPA}]^{2-}$, [Fe-EDDA] described in this paper, and $[\text{Fe-EDTA}]^-$ (Baichoo & Heyduk, 1997) were very similar. This indicates that proteolysis by these iron–chelate complexes is independent of their charge, as would be expected for cleavage by diffusible hydroxyl radicals. Previous studies have shown that proteolysis by $[\text{Fe-EDTA}]^-$ is determined primarily by solvent accessibility (Ermacora et al., 1994). Thus, in protein footprinting experiments performed using these chelates, any changes in susceptibility to proteolysis will most likely di-

rectly reflect changes in a local solvent accessibility. Results obtained with $[Fe\text{-}HDFO]^+$ and with $[(OP)_2Cu]^+$ showed that in addition to cAMP-induced changes observed using $[Fe\text{-}DTPA]^{2-}$, [Fe-EDDA], and $[Fe\text{-}EDTA]^-$, other regions of CRP were found to be affected by cAMP. $[Fe\text{-}HDFO]^+$ and $[(OP)_2Cu]^+$ share several physicochemical properties that differentiate them from the remaining chelates studied in this paper. Both $[Fe\text{-}HDFO]^+$ and $[(OP)_2Cu]^+$ are positively charged, are larger in size compared to chelates from EDTA family, and the mechanism of proteolysis by these chelates may also be different from the chelates from EDTA family. Electrochemical studies have demonstrated that although $[Fe\text{-}HDFO]^+$ can generate hydroxyl radicals (Borg & Schaich, 1986), the cycling of Fe^{3+} to Fe^{2+}, which is necessary to perpetuate the reaction, is decreased when ascorbate is used as a reducing agent due to the high affinity of DFO for Fe^{3+} (Borg & Schaich, 1984). $[(OP)_2Cu]^+$-mediated proteolysis was proposed to act through a copper-oxo intermediate (Bateman et al., 1985; Wu et al., 1995; Gallagher et al., 1998). $[(OP)_2Cu]^+$ has been used extensively as a nuclease and binds to specific sites on DNA (Schaeffer et al., 1996). $[(OP)_2Cu]^+$ may also preferentially bind to particular sites on proteins. The observation of highly preferred sites in CRP for the cleavage with $[(OP)_2Cu]^+$ is consistent with this possibility. Positive charge seems to be the least likely reason for the difference in the results obtained with $[(OP)_2Cu]^+$, $[Fe\text{-}HDFO]^+$, and iron-chelates from the EDTA family because within the EDTA family the charge of the chelate was apparently not very important. The larger size of $[(OP)_2Cu]^+$ and $[Fe\text{-}HDFO]^+$ could result in detecting more global conformational changes, which would not produce significant changes in the local solvent accessibility, and thus would remain undetected by EDTA family chelates. A rigid domain movement could be an example of such conformational change. Similarly, the ability of $[(OP)_2Cu]^+$ to bind to macromolecule before the cleavage could also result in an increased sensitivity of this protease to small changes of the protein surface that would not result in significant changes in solvent accessibility and, thus, would escape detection by EDTA family chelates.

In summary, the results described here provide a detailed map of regions of CRP affected by binding of cyclic nucleotides. Also our results show that combined use of proteases of different size, charge, and hydrophobicity for protein footprinting gives a more complete picture of structural changes than any single protease alone.

Materials and methods

Materials

$HMPK\text{-}CRP\text{-}His_6$ was over expressed, purified, and shown to be as active as wt CRP in binding cAMP, DNA sequences, and RNA polymerase, as described previously (Baichoo & Heyduk, 1997). Desferrioxamine mesylate and DTPA were from Sigma (St. Louis, Missouri). EDDA was from Fluka (Buchs, Switzerland). Cupric sulfate pentahydrate, *o*-phenanthroline monohydrate, 3-mercaptopropionic acid, and neocuproine all were from Fluka. Hydrogen peroxide (30% wt) and ammonium iron (II) sulfate hexahydrate were from Aldrich (Milwaukee, Wisconsin). Nickel(II)-NTA-agarose was from Qiagen (Chatsworth, California). Gamma ^{33}P-ATP was from Andotek (Irvine, California). All other reagents were from Sigma.

Phosphorylation of $HMPK\text{-}CRP\text{-}His_6$

$HMPK\text{-}CRP\text{-}His_6$ was labeled with ^{33}P in a reaction mixture containing 38 μM CRP derivative, 500 U of bovine heart muscle cAMP-dependent protein kinase catalytic subunit, 0.27 μM [γ^{33}P]ATP (250 μCi), 30 mM $MgCl_2$, and 66 mM DTT with 20 mM Tris-HCl (pH 7.5), 100 mM NaCl buffer to a final volume of 300 μL. The reaction was carried out for 1 h at 37 °C, after which 40 μL of Ni^{2+}–NTA–agarose suspension was added. The reaction was incubated at room temperature for 15 min with gentle shaking, after which it was centrifuged (2 min at 1,000 × *g*, 4 °C) and the supernatant discarded. The Ni^{2+}–NTA–agarose bead pellet was resuspended in 20 mM Tris-HCl (pH 7.5), 100 mM NaCl buffer (200 μL). After washing the pellet twice in buffer, the ^{33}P-labeled $HMPK\text{-}CRP\text{-}His_6$ was eluted by suspending the Ni^{2+}–NTA–agarose beads in 20 mM Tris-HCl (pH 7.5), 100 mM NaCl, 0.5 M imidazole buffer (200 μL) with gentle shaking at room temperature for 15 min. The resulting suspension was centrifuged (2 min at 1,000 × *g*, 4 °C), and the supernatant was collected and dialyzed overnight at 4 °C against 10 mM MOPS-NaOH (pH 7.2), 250 mM NaCl, and 10 mM $MgCl_2$, and stored at 4 °C.

$[Fe\text{-}DTPA]^{2-}$, [Fe-EDDA], and $[Fe\text{-}HDFO]^+$ footprinting reactions

Reaction mixtures contained 4–9 μM $CRP^{\#}$ dimer, 1.3 mM chelate, 0.6 mM $(NH_4)Fe^{II}(SO_4)_2$, 1 mM H_2O_2, 20 mM sodium ascorbate, and 10 mM MOPS-NaOH (pH 7.2), 250 mM NaCl, 10 mM $MgCl_2$ buffer to a final volume of 10 μL. When present, cAMP and cGMP were at 400 μM. Each chelate was prepared as a 40 mM stock solution (pH adjusted to 7.2 by NaOH) and stored at −20 °C. All other reagents were prepared immediately prior to use. Reactions were started by simultaneous addition of chelate and $(NH_4)Fe^{II}(SO_4)_2$ [as a freshly prepared 13.3 mM chelate–6.6 mM $(NH_4)Fe^{II}(SO_4)_2$ mixture], H_2O_2, and sodium ascorbate. Reactions were terminated after 40 min by the addition of 5 μL of 3× sample buffer [150 mM Tris-HCl (pH 7.9), 36% glycerol, 12% SDS, 6% β-mercaptoethanol, and 0.01% bromophenol blue].

$[(OP)_2Cu]^+$ footprinting reactions

Stock solutions of 0.1 M $CuSO_4$, 0.4 M *o*-phenanthroline (OP) (in ethanol), 0.058 M 3-mercaptoproprionic acid (MPA), and 40 mM neocuproine (in ethanol) were all prepared just prior to use. Stock solutions of $[(OP)_2Cu]^+$ were prepared at 150 μM $CuSO_4$ and 2 mM OP, respectively. Reaction mixtures (7 μL) contained 5–10 μM $CRP^{\#}$ dimer, 400 μM cAMP, or cGMP when present. Reactions were brought to final volume by 10 mM MOPS-NaOH (pH 7.2), 250 mM NaCl, and 10 mM $MgCl_2$. Cleavage was initiated by addition of aqueous $(OP)_2Cu^+$ and MPA resulting in final concentrations of 6.0 μM Cu^{2+}, 77 μM OP, and 2.26 mM MPA. Reactions using 5-, 10-, and 25-fold increases in concentrations of OP and $CuSO_4$ yielded identical results that were incorporated into the data set for subsequent analyses. Reactions were allowed to proceed for 30 min at room temperature, after which they were stopped by adding neocuproine to a final concentration of 1.6 mM. Seven microliters of 3× sample buffer [150 mM Tris-HCl (pH 7.9), 36% glycerol, 12% SDS, 6% β-mercaptoethanol, and 0.01% bromophenol blue] were then added. For all proteases used, cleavage products were resolved on 16 cm × 14 cm × 0.75 mm tricine-

SDS–polyacrylamide gels (Schagger & von Jagow, 1987; Heyduk & Heyduk, 1994). Gels were dried, and their digital images were obtained with a Molecular Dynamics Model 425B Phosphorimager. Molecular weight markers and assignment of cleavage sites were performed as described previously (Baichoo & Heyduk, 1997.)

Data analysis

Data were analyzed as described previously (Heyduk et al., 1996). In short, full-width scanning of each lane yielded phosphorimager intensities plotted vs. electrophoretic mobility using ImageQuant (Molecular Dynamics, Sunnyvale, California). Intensity plots were aligned to correct for smiling or frowning of bands between lanes using ALIGN [available on request; written in BASIC and running under LabWindows (National Instruments)]. After alignment, intensity plots were imported into SigmaPlot (Jandel Scientific, Austin, Texas), where correction for gel-loading efficiencies, transformation of electrophoretic mobility of fragments to positions of amino acid residues, and preparation of difference plots were performed using routines written in SigmaPlot transform language (available on request). After analysis, data were presented as a difference plot that shows $(I - I_{CRP\#})/I$ where I is the corrected Phosphorimager intensity for the complex under study, and $I_{CRP\#}$ is the corrected Phosphorimager intensity for uncomplexed CRP$^{\#}$.

Acknowledgment

This work was supported by a NIH Grant GM50514.

References

Adhya S, Ryu S, Garges S. 1995. Role of allosteric changes in cyclic AMP receptor protein function. *Subcell Biochem 24*:303–321.

Angulo JA, Krakow JS. 1985. Effect of deoxyribopolymers and ribopolymers on the sensitivity of the cyclic-AMP receptor protein of *Escherichia coli* to proteolytic attack. *Arch Biochem Biophys 236*:11–16.

Baichoo N, Heyduk T. 1997. Mapping conformational changes in a protein—Application of a protein footprinting technique to cAMP-induced conformational changes in cAMP receptor protein. *Biochemistry 36*:10830–10836.

Bateman RC Jr, Youngblood WW, Busby WH Jr, Kizer JS. 1985. Nonenzymatic peptide alpha-amidation. Implications for a novel enzyme mechanism. *J Biol Chem 260*:9088–9091.

Borg DC, Schaich KM. 1984. Cytotoxicity from coupled redox cycling of autooxidizing xenobiotics and metals. *Israel J Chem 24*:38–53.

Borg DC, Schaich KM. 1986. Prooxidant action of desferrioxamine: Fenton-like production of hydroxyl radicals by reduced ferrioxamine. *J Free Radic Biol Med 2*:237–243.

Brenowitz M, Senear DF, Shea MA, Ackers GK. 1986. Quantitative DNase footprint titration: A method for studying protein–DNA interactions. *Methods Enzymol 130*:132–181.

Cheng X, Gonzalez ML, Lee JC. 1993. Energetics of intersubunit and intrasubunit interactions of *Escherichia coli* adenosine cyclic 3′,5′-phosphate receptor protein. *Biochemistry 32*:8130–8139.

Cheng X, Kovac L, Lee JC. 1995. Probing the mechanism of CRP activation by site-directed mutagenesis: The role of serine 128 in the allosteric pathway of cAMP receptor protein activation. *Biochemistry 34*:10816–10826.

Cheng X, Lee JC. 1998. Interactive and dominant effects of residues 128 and 141 on cyclic nucleotide and DNA bindings in *Escherichia coli* cAMP receptor protein. *J Biol Chem 273*:705–712.

DeGrazia H, Harman JG, Tan GS, Wartell RM. 1990. Investigation of the cAMP receptor protein secondary structure by Raman spectroscopy. *Biochemistry 29*:3557–3562.

Ebright RH, Le Grice SF, Miller JP, Krakow JS. 1985. Analogs of cyclicAMP that elicit the biochemically defined conformational change in catabolite gene activator protein (CAP) but do not stimulate binding to DNA. *J Mol Biol 182*:91–107.

Eilen E, Krakow JS. 1977. Cyclic AMP-mediated intersubunit disulfide cross-linking of the cyclic AMP receptor protein of *Escherichia coli*. *J Mol Biol 114*:47–60.

Ermacora MR, Ledman DW, Hellinga HW, Hsu GW, Fox RO. 1994. Mapping staphylococcal nuclease conformation using an EDTA-Fe derivative attached to genetically engineered cysteine residues. *Biochemistry 33*:13625–13641.

Fried MG, Crothers DM. 1984. Equilibrium studies of the cyclic AMP receptor protein-DNA interaction. *J Mol Biol 172*:241–262.

Gallagher J, Zelenko O, Walts AD, Sigman DS. 1998. Protease activity of 1,10-phenanthroline-copper(I)–targeted scission of the catalytic site of carbonic anhydrase. *Biochemistry 37*:2096–2104.

Garges S, Adhya S. 1988. Cyclic AMP-induced conformational change of cyclic AMP receptor protein (CRP): Intragenic suppressors of cyclic AMP-independent crp mutations. *J Bacteriol 170*:1417–1422.

Garges S, Adhya S. 1985. Sites of allosteric shift in the structure of the cyclic AMP receptor protein. *Cell 41*:745–751.

Heyduk E, Heyduk T. 1994. Mapping protein domains involved in macromolecular interactions: A novel protein footprinting approach. *Biochemistry 33*: 9643–9650 [Erratum. 1995. *Biochemistry 34*:1538].

Heyduk T, Heyduk E, Severinov K, Tang H, Ebright RH. 1996. Determinants of RNA polymerase alpha subunit for interaction with beta, beta′, and sigma subunits: Hydroxyl-radical protein footprinting. *Proc Natl Acad Sci USA 93*:10162–10166.

Heyduk T, Lee JC. 1989. *Escherichia coli* cAMP receptor protein: Evidence for three protein conformational states with different promoter binding affinities. *Biochemistry 28*:6914–6924.

Hinds MG, King RW, Feeney J. 1992. 19F N.M.R studies of conformational changes accompanying cyclic AMP binding to 3-fluorophenylalanine-containing cyclic AMP receptor protein from *Escherichia coli*. *Biochem J 287*:627–632.

Kim J, Adhya S, Garges S. 1992. Allosteric changes in the cAMP receptor protein of *Escherichia coli*: Hinge reorientation. *Proc Natl Acad Sci USA 89*:9700–9704.

Kolb A, Busby S, Buc H, Garges S, Adhya S. 1993. Transcriptional regulation by cAMP and its receptor protein. *Annu Rev Biochem 62*:749–795.

Krakow JS, Pastan I. 1973. Cyclic adenosine monophosphate receptor: Loss of cAMP-dependent DNA binding activity after proteolysis in the presence of cyclic adenosine monophosphate. *Proc Natl Acad Sci USA 70*:2529–2533.

Kraulis PJ. 1991. MOLSCRIPT: A program to produce both detailed and schematic plots of protein structures. *J Appl Crystallogr 24*:946–950.

Lee BJ, Lee SJ, Hayashi F, Aiba H, Kyogoku Y. 1990. A nuclear magnetic resonance study of the cyclic amp receptor protein (CRP): Assignments of the NH protons of histidine and tryptophan residues and the effect of binding of cAMP to CRP. *J Biochem (Tokyo) 107*:304–309.

McKay DB, Weber IT, Steitz TA. 1982. Structure of catabolite gene activator protein at 2.9-A resolution. Incorporation of amino acid sequence and interactions with cyclic AMP. *J Biol Chem 257*:9518–9524.

Nicholls A, Sharp KA, Honig B. 1991. Protein folding and association: Insights from the interfacial and thermodynamic properties of hydrocarbons. *Proteins 11*:281–296.

Pampeno C, Krakow JS. 1979. Cross-linking of the cAMP receptor protein of *Escherichia coli* by *o*-phenylenedimaleimide as a probe of conformation. *Biochemistry 18*:1519–1525.

Parkinson G, Wilson C, Gunasekera A, Ebright YW, Ebright RE, Berman HM. 1996. Structure of the CAP-DNA complex at 2.5 Angstroms resolution: A complete picture of the protein-DNA interface. *J Mol Biol 260*:395–408.

Passner JM, Steitz TA. 1997. The structure of a CAP-DNA complex having two cAMP molecules bound to each monomer. *Proc Natl Acad Sci USA 94*:2843–2847.

Ryu S, Kim J, Adhya S, Garges S. 1993. Pivotal role of amino acid at position 138 in the allosteric hinge reorientation of cAMP receptor protein. *Proc Natl Acad Sci USA 90*:75–79.

Schaeffer F, Rimsky S, Spassky A. 1996. DNA-stacking interactions determine the sequence specificity of the deoxyribonuclease activity of 1,10-phenanthroline-copper ion. *J Mol Biol 260*:523–539.

Schagger H, von Jagow G. 1987. Tricine-sodium dodecyl sulfate-polyacrylamide gel electrophoresis for the separation of proteins in the range from 1 to 100 kDa. *Anal Biochem 166*:368–379.

Schultz SC, Shields GC, Steitz TA. 1991. Crystal structure of a CAP-DNA complex: The DNA is bent by 90 degrees. *Science 253*:1001–1007.

Sixl F, King RW, Bracken M, Feeney J. 1990. 19F-N.M.R Studies of ligand binding to 5-fluorotryptophan- and 3-fluorotyrosine-containing cyclic AMP receptor protein from *Escherichia coli*. *Biochem J 266*:545–552.

Takahashi M, Blazy B, Baudras A. 1980. An equilibrium study of the cooperative binding of adenosine cyclic 3′,5′-monophosphate and guanosine cyclic 3′,5′-monophosphate to the adenosine cyclic 3′,5′-monophosphate receptor protein from *Escherichia coli*. *Biochemistry 19*:5124–5130.

Tan GS, Kelly P, Kim J, Wartell RM. 1991. Comparison of cAMP receptor

protein (CRP) and a cAMP-independent form of CRP by Raman spectroscopy and DNA binding. *Biochemistry 30*:5076–5080.

Tsugita A, Blazy B, Takahashi M, Baudras A. 1982. A characterization by sequencing of the termini of the polypeptide chain of cyclic AMP receptor protein from *Escherichia coli* and the subtilisin produced N-terminal fragment. *FEBS Lett 144*:304–308.

Weber IT, Steitz TA. 1987. Structure of a complex of catabolite gene activator protein and cyclic AMP refined at 2.5 A resolution. *J Mol Biol 198*:311–326.

Wu CW, Wu FY. 1974. Conformational transitions of cyclic adenosine monophosphate receptor protein of *Escherichia coli*. A temperature-jump study. *Biochemistry 13*:2573–2578.

Wu FY, Nath K, Wu CW. 1974. Conformational transitions of cyclic adenosine monophosphate receptor protein of *Escherichia coli*. A fluorescent probe study. *Biochemistry 13*:2567–2572.

Wu J, Perrin DM, Sigman DS, Kaback HR. 1995. Helix packing of lactose permease in *Escherichia coli* studied by site-directed chemical cleavage. *Proc Natl Acad Sci USA 92*:9186–9190.